

Received: 28.02.2025

Accepted: 13.04.2025

Research Article

Computational Chemistry Methods for Molecular Analysis and In Silico Investigation of Platinum (IV) Complexes

Saadet KAYA¹, Sultan ERKAN

Chemistry Department, Science Faculty, Sivas Cumhuriyet University, 58140, Sivas, Turkey

Abstract: Computational chemistry methods were used to investigate the six-coordinated Pt1, Pt2 and Pt3 complexes at the molecular level and to determine their advantages over the four-coordinated complexes. The most suitable calculation level was determined by benchmark analysis using experimental bond lengths and the WB97XD/6-31G(d,p)/SDD method was selected. IR, 1H- and 13C-NMR spectroscopic data were calculated for the structural analysis of Pt1-Pt3 complexes and compared with experimental findings. HOMO and LUMO contour diagrams and molecular electrostatic potential (MEP) maps were created to understand the electron transfer potential of the complexes. This information provides important clues in predicting their interactions with biological receptors. Molecular docking studies were performed to evaluate the comparative biological activities of the studied platinum (IV) complexes (Pt1-Pt3) with platinum (II) complexes, one of the current chemotherapy agents. Pt1-Pt3 complexes were docked with breast cancer (PDB ID: 1JNX), lung cancer (PDB ID: 1X2J) and colon cancer (PDB ID: 2HQ6) proteins. As a result of the investigations, it was determined that these complexes were superior in terms of anticancer activity compared to the reference complex (cis-Pt).

Keywords: Platinum (IV) Complexes, anticancer, docking

1. Introduction

Pt (II) complexes, which are accepted as FDA-approved platinum-based anticancer drugs, are widely used in the treatment of cancer patients receiving chemotherapy. [1] However, Pt (II) complexes used as anticancer drugs have some negative side effects. These can be listed as drug resistance, dose-limiting toxic side effects, short-term retention in the bloodstream, and systemic side effects. [1,2] A new Pt (IV) prodrug has been developed in order to reduce the negative side effects of Pt (II) drugs. As a result of the oxidation of the Pt (II) precursor with square planar geometry, Pt (IV) complexes with octahedral geometry are formed by gaining two axial ligands and Pt (IV) is reduced to Pt (II). In addition, these added ligands can be coordinated during intracellular reduction. [1]. Pt (IV) drugs are chemically less active than Pt (II) drugs. The biggest advantage of this low chemical activity is that it helps to provide more

effect at lower doses. The fact that Pt(IV) drugs are more inert than Pt(II) drugs allows them to be more effective at lower doses, which is one of their most important advantages. This feature prevents the side effects of Pt(IV) drugs from reaching the target cancer cell. [3,4] The main Pt(II) drugs (e.g., cisplatin), which are widely used in various multifunctional Pt(IV) complexes, can be made more functional by replacing the leaving groups in the d8 square-planar Pt(II) complex with bioactive ligands. This structural change allows the multifunctional Pt(IV) complexes to be reduced intracellularly to Pt(II) forms and simultaneously release the bioactive ligands from axial positions. Platinum-based drugs have also been associated with resistance through mechanisms such as decreased cellular uptake, increased excretion of platinum from the cell, early interaction with biomolecules that cause inactivation, increased DNA repair capacity, and abnormal apoptotic

¹ Corresponding Authors

e-mail: saadetskaya58@gmail.com

processes. [20], [21], [22], [23], [24], [25], [26], [27]. In order to overcome these limitations and improve the selectivity and pharmacokinetics of traditional platinum drugs while reducing side effects and resistance issues, researchers have investigated Pt(IV) complexes with octahedral structures that exceed the classical structure of cisplatin. Some of these prodrugs can be administered orally, which cisplatin analogs cannot. In addition, the two additional Pt coordination sites, R1 and R2, in these compounds provide more opportunities for functional modification (Figure 1). By selecting suitable ligands, properties such as reduction rate, lipophilicity, targeting ability, and potential for synergistic cancer treatment with other small molecule drugs can be adjusted. In addition, nanoscale drug delivery methods have attracted attention in recent years due to innovative research on different materials. This method provides stable and long-term delivery of chemotherapeutics, as well as multidrug and multimodal synergistic treatment opportunities [28]. More importantly, Pt(IV) prodrugs can be more easily absorbed by various nanocarriers than cisplatin analogs due to their switchable properties. By adjusting the leaving and non-leaving groups in the planar structure of platinum analogs, second-generation platinum drugs have shown improved metabolic dynamics and structural changes in Pt-DNA adducts, contributing to reduced side effects and broadening the anticancer spectrum. As an alternative to the planar structures of cisplatin analogs, Pt(IV) complexes with octahedral structures not only do not exhibit kinetic inertia, but also reduce interactions with circulating biomolecules, offering new opportunities for replacing more functional axial ligands. In general, Pt(IV) prodrugs undergo a reduction step known as the 'activation' process in the patient's body and are converted into Pt(II) drugs that exhibit natural cytotoxic effects. Therefore, the reducing potential of Pt(IV) complexes is an important element to be considered at the design stage. Furthermore, potential influencing factors are thought to be related to axial ligands with stronger electron-withdrawing ability capable of enhancing hydrolysis [5]. Since the 1980s, interest in Pt(IV) complexes has been steadily increasing. In this field, Von Zelewsky (8) and later Swager (9)

successfully synthesized various six-coordinated Pt(IV) products in the form of Pt(IV). Various research groups, such as Rourke and co-workers (11), Bruce and co-workers (12), Ionescu and co-workers (13), have carried out studies on the synthesis of six-coordinated complexes of platinum. In the context of photophysical properties and applications in light-emitting electrochemical cells (LEECs), the photophysical properties of Pt(IV) complexes have been studied in detail by Jenkins and Bernhard (14) and González-Herrero and co-workers (15) [6].

This study aims to comprehensively investigate the structural properties, biological activities and interactions of six-coordinated Pt(IV) complexes, Pt1, Pt2 and Pt3 [7,8], with biological receptors using computational chemistry methods. Benchmark analysis determined that the WB97XD/6-31G(d,p)/SDD method was the most suitable calculation level by utilizing experimental bond lengths. IR, ¹H- and ¹³C-NMR spectroscopic data were calculated and compared with experimental results. In addition, electron transfer potential of these complexes was visualized using HOMO-LUMO contour diagrams and molecular electrostatic potential (MEP) maps. The study evaluated the interactions of Pt1-Pt3 complexes with biological receptors using molecular docking analysis; during this process, the complexes were docked with breast cancer (PDB ID: 1JNX), lung cancer (PDB ID: 1X2J) and colon cancer (PDB ID: 2HQ6) proteins. The findings revealed that Pt(IV) complexes are superior in terms of anticancer activity compared to the reference platinum(II) complex, cisplatin. This approach aims to contribute to the development of new strategies to increase the therapeutic potential of Pt(IV) complexes.

2. Computational Method

The molecular structures of Pt1, Pt2 and Pt3 complexes were designed with GaussView 6.0.16 program [25]. The structures were first optimized with the Ultra Force Field (UFF) method, a molecular mechanics method [26]. Then, full optimization was performed at B3LYP/6-31G(d,p)/LANL2DZ, M062X/6-31G(d,p)/LANL2DZ, WB97XD/6-31G(d,p)/LANL2DZ, B3LYP/6-31G(d,p)/SDD, M062X/6-31G(d,p)/SDD, WB97XD/6-

31G(d,p)/LANL2DZ and WB97XD/6-31G(d,p)/SDD level with Gaussian 16: ES64L-G16RevC.01 program in gas phase [27] and no imaginary frequency was obtained [28]. Here, B3LYP, M062X and WB97XD are a hybrid density functional theory (DFT) method [30], 6-31G(d)/LANL2DZ and 6-31G(d,p)/SDD are a mixed basis set. The LANL2DZ basis set including effective core potential is used to model the central atom platinum orbitals, and the polarized basis set 6-31G(d) is used to model the orbitals of other atoms [31]. In order to estimate the first hyperpolarizability, d polarization functions are added to the carbon and nitrogen atoms [32]. In this study, the experimental structure parameters of Pt1 complex and the structure parameters calculated at B3LYP/6-31G(d,p)/LANL2DZ, M062X/6-31G(d,p)/LANL2DZ, WB97XD/6-31G(d,p)/LANL2DZ, B3LYP/6-31G(d,p)/SDD, M062X/6-31G(d,p)/SDD, WB97XD/6-31G(d,p)/LANL2DZ and WB97XD/6-31G(d,p)/SDD levels were benchmarked. The most appropriate calculation

level was determined as WB97XD/6-31G(d,p)/SDD. The ground state structures, structure parameters and IR spectra of the complexes were obtained. To support the ground state structures of the complexes, ¹H-NMR spectra were calculated by gauge-including atomic orbital (GIAO) approach [29]. ¹H-NMR and chemical shift values are given according to TMS reference. Anticancer activities against quadruplicate-coordinated platinum complexes were investigated by molecular docking in silico method.

3. Results and discussion

3.1. Optimized Structures

The optimized structures of Pt1-Pt3 complexes are the lowest potential energy states of geometric structures with spatial decompositions. Geometric optimizations of the complexes were obtained at all computational levels. All of the geometric optimizations obtained are ground state structures. Optimized structures and their labels obtained with WB97XD/6-31G(d,p)/SDD levels for Pt1-Pt3 complexes are given in Figure 1.

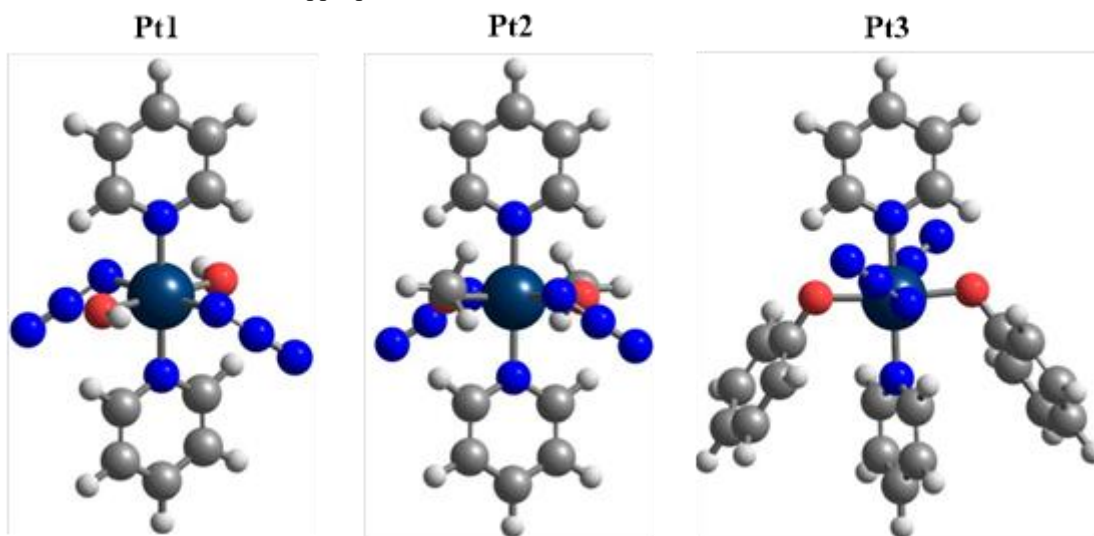


Figure 1. Optimized structures of Pt1-Pt3 complexes.

Table 1. Experimental and calculated bond lengths of Pt1 complex by some methods.

Bonds (Å)	B3LYP		M062X		WB97XD		Exp.
	LANL2DZ	SDD	LANL2DZ	SDD	LANL2DZ	SDD	
Pt–N6	2.107	2.0977	2.0790	2.0720	2.0788	2.072	2.046
N6–N7	1.2225	1.2221	1.2193	1.2194	1.2191	1.219	1.215
N7–N8	1.1535	1.1536	1.1412	1.1412	1.1451	1.1451	1.140
Pt–N9	2.1070	2.0977	2.0790	2.0719	2.0788	2.0725	2.043
N9–N10	1.2225	1.2221	1.2193	1.2194	1.2191	1.2190	1.218
N10–N11	1.1535	1.1536	1.1412	1.1412	1.1451	1.1451	1.146
Pt–O2	2.0469	2.0421	2.0174	2.0141	2.0266	2.0229	1.990
Pt–O4	2.0469	2.0421	2.0174	2.0141	2.0266	2.0229	2.027
Pt–N12	2.0698	2.0798	2.0613	2.0616	2.0632	2.0644	2.046

Saadet KAYA, Sultan ERKAN

Pt-N23	2.0697	2.0630	2.0342	2.0362	2.0381	2.0423	2.047
R²	0.9987	0.9990	0.9987	0.9990	0.9989	0.9992	-

3.2. Benchmark Analysis and Structural Characterization

Benchmark analysis is a type of analysis performed to determine the most appropriate calculation level. Different calculation levels are determined according to the properties of the structures and are performed by comparing the experimental value with the calculated value. The calculation level with the correlation coefficient (R2) values closest to one is preferred. The experimental crystal structure data of platinum complexes were compared with the bond lengths and bond angles calculated at different levels. As analysis methods, B3LYP/6-31G(d,p)/LANL2DZ, M062X/6-31G(d,p)/LANL2DZ, WB97XD/6-31G(d,p)/LANL2DZ, B3LYP/6-31G(d,p)/SDD, M062X/6-31G(d,p)/SDD, WB97XD/6-31G(d,p)/LANL2DZ

and WB97XD/6-31G(d,p)/SDD levels were determined. The calculated bond lengths and bond angles for the Pt1-Pt3 complex are given in Table 1 together with the experimental values.

The calculated bond lengths are compared with the experimentally obtained bond lengths. The calculated and experimentally obtained values and correlation coefficients R2 are shown in detail in Table 1. In order to determine the calculation level for Pt1, the correlation number must be close to or equal to one. When Table 1 was examined, it was determined that the value closest to one was WB97XD/6-31G(d,p)/SDD [9,10]. The structural parameters of the studied complexes calculated with the WB97XD/6-31G(d,p)/SDD level are given in Table 2.

Table 2. Calculated structural parameters of Pt1, Pt2 and Pt3 complexes

Bond	Pt1	Pt2	Pt3
Pt-N27	2.0723	Pt-N25	2.07857
N27-N28	1.2190	N25-N26	1.218
N28-N30	1.1451	N26-N28	1.14571
Pt-N26	2.0725	Pt-N24	2.07857
N26-N29	1.2190	N24-N27	1.21800
N29-N31	1.1451	N27-N29	1.14571
Pt-O22	2.0229	Pt-O22	2.03101
Pt-O24	2.0229	Pt-O23	2.03101
Pt-N32	2.0644	Pt-N30	2.06312
Pt-N33	2.0423	Pt-N31	2.04202
Pt-N23		Pt-N22	2.07916
N23-N24		N22-N25	1.21973
N24-N26		N25-N27	1.14414
N25-N26		Pt-O30	2.04710
N26-N28		Pt-O31	2.04697
N27-N29		Pt-N28	2.07344
N28-N30		Pt-N29	2.07783
N29-N31			
Angle (°)			
N27-Pt-N25	176.0	N30-Pt-N31	179.99967
N32-Pt-N33	180	N24-Pt-N25	176.26346
O22-Pt-O24	179.4	O22-Pt-O23	179.30763
O22-Pt-N27	89.0	C36-O22-Pt	117.90688
O22-Pt-N25	90.9	N25-Pt-O23	86.16931
N32-Pt-N27	92.0	N24-Pt-O22	86.16896
N33-Pt-N26	88.0	N30-Pt-N25	91.86832
-	-	N24-Pt-N31	88.13170
Dihedral Angle (°)			
N28-N27-N26-N29	101.47699	N26-N25-N24-N27	103.20592
Pt-N26-N29-N31	174.62393	Pt-N24-N27-N29	171.98194
Pt-N27-N28-N30	174.60474	Pt-N25-N26-N28	172.01707
		N24-N23-N22-N25	107.45051
		Pt-N22-N25-N27	168.54269
		Pt-N23-N24-N26	168.86862

According to the data obtained from Table 2, the bonding of hydroxyl, methoxy and phenol groups did not significantly change the bond lengths, bond angles and dihedral angles around the central

platinum atom. Pt-N bond lengths were calculated as approximately 2.07 Å in all complexes. Pt-O bond lengths for Pt1, Pt2 and Pt3 complexes were determined as 2.02, 2.03 and 2.04 Å, respectively,

while N=N bond lengths were around 1.21 and 1.14 Å. N–Pt–N and O–Pt–O bond angles exhibited ideal trans angles of approximately 180°, while O–Pt–N bond angles were calculated as approximately 90°. These results show that the central platinum atom has an octahedral geometry. In terms of dihedral angles, the calculated values for N28–N27–N26–N29, Pt–N26–N29–N31 and Pt–N27–N28–N30 were found to be 101.48°, 174.62° and 174.60°, respectively. Experimentally, these angles were measured as 119.5°, 175.7° and 177.9°, respectively, which shows high agreement with the calculated values. This agreement between the calculation and experimental results supports the accuracy of the method used. In addition, the fact that the bond lengths, bond angles and dihedral angles on one side of the complexes are equal to the values on the other side clearly reveals that these complexes have a center of symmetry.

3.3. IR spectra and labeling of characteristic peaks

IR spectroscopy is one of the most important techniques used in molecular structure characterization, allowing the analysis of the frequencies of peaks in the spectrum created by vibrations characteristic of a molecule. In this study, the IR spectra of the designed Pt1–Pt3 complexes were calculated at the WB97XD/6-31G(d,p)/SDD level. The IR spectra of the complexes, the frequencies of the characteristic peaks and their labeling are presented in Figure 2. As seen in Figure 2, the characteristic Caro-H and Cali-H bond stresses for the complexes are in the range of 3300–3200 cm⁻¹. In addition, the characteristic N=N bond stress was observed at a frequency of approximately 2200 cm⁻¹ in all complexes, and this peak stands out as the most intense peak with high oscillator strength. In addition, C=C bond stresses were determined around 1600 cm⁻¹.

In-plane and out-of-plane vibrations of the complexes such as Wagging (ω), Scissoring (δ), Rocking (ρ) and Twisting (τ) were observed in the range of 1000–700 cm⁻¹. Apart from this, the bond stresses at approximately 500 cm⁻¹ correspond to Pt–O bonds, and the bond stresses at 400 cm⁻¹ correspond to Pt–N bonds. There is no scaling factor in the literature for the conversion of harmonic frequencies to anharmonic frequencies

for the calculation method WB97XD/6-31G(d,p)/SDD. In addition, the experimental bond stress frequencies of the complexes are not available in the literature. However, the findings obtained within the scope of this study can provide useful reference information for similar synthesized compounds.

3.4. NMR spectra and chemical shift values

Nuclear magnetic resonance (NMR) spectroscopy is one of the most important methods used in molecular structure determination. With this technique, ¹H-NMR and ¹³C-NMR chemical shift values of the molecule are measured, and results are generally obtained according to the TMS reference. Important information about the structural properties of the molecule is obtained from these chemical shift values. In this study, ¹H-NMR spectra of the designed Pt(IV) complexes were calculated by the GIAO method and WB97XD/6-31G(d,p)/SDD level. At the same level, the shielding value for TMS protons was found to be 32.8599 ppm and the chemical shift values were calculated using Equation (1):

$$\delta H = \sum H_{TMS} - \sum H_{sample} \quad (1)$$

Here $\sum H_{TMS}$ is the shielding of TMS protons and $\sum H_{sample}$ is the shielding of sample protons. ¹H-NMR spectra of the complexes, labeling of peaks and ¹H-NMR chemical shift values are given in Figure 3.

Figure 3 shows the ¹H-NMR chemical shifts and molecular structures of Pt1, Pt2 and Pt3 complexes. These spectra visualize the chemical shift values of the protons of the complexes in different binding environments and relate this information to the molecular structures. In all complexes, the chemical shift values of the protons attached to the aromatic ring are between 8–12 ppm. These shift values indicate that the shielding of these protons is low due to the decrease in the electron density of the aromatic system and therefore they have higher chemical shift values. The chemical shifts of the aromatic protons in this range indicate that the aromatic rings of the complexes do not interact directly with the platinum atom, but the aromatic structures of the ligands are preserved. The chemical shift values around 4–6 ppm observed in the Pt2 complex belong to the aliphatic CH₃ groups. The chemical shift values of these protons are due to the relatively high electron density around the

Saadet KAYA, Sultan ERKAN

aliphatic groups. This situation shows that the electron-withdrawing effect of the aliphatic groups in the Pt2 complex is low. The chemical shift values of the hydrogens bonded to the oxygen atom in the

Pt1 complex are around 1.66 ppm. The hydrogen atoms bonded to oxygen, which is an electronegative atom, have a low chemical shift value because they undergo a screening effect.

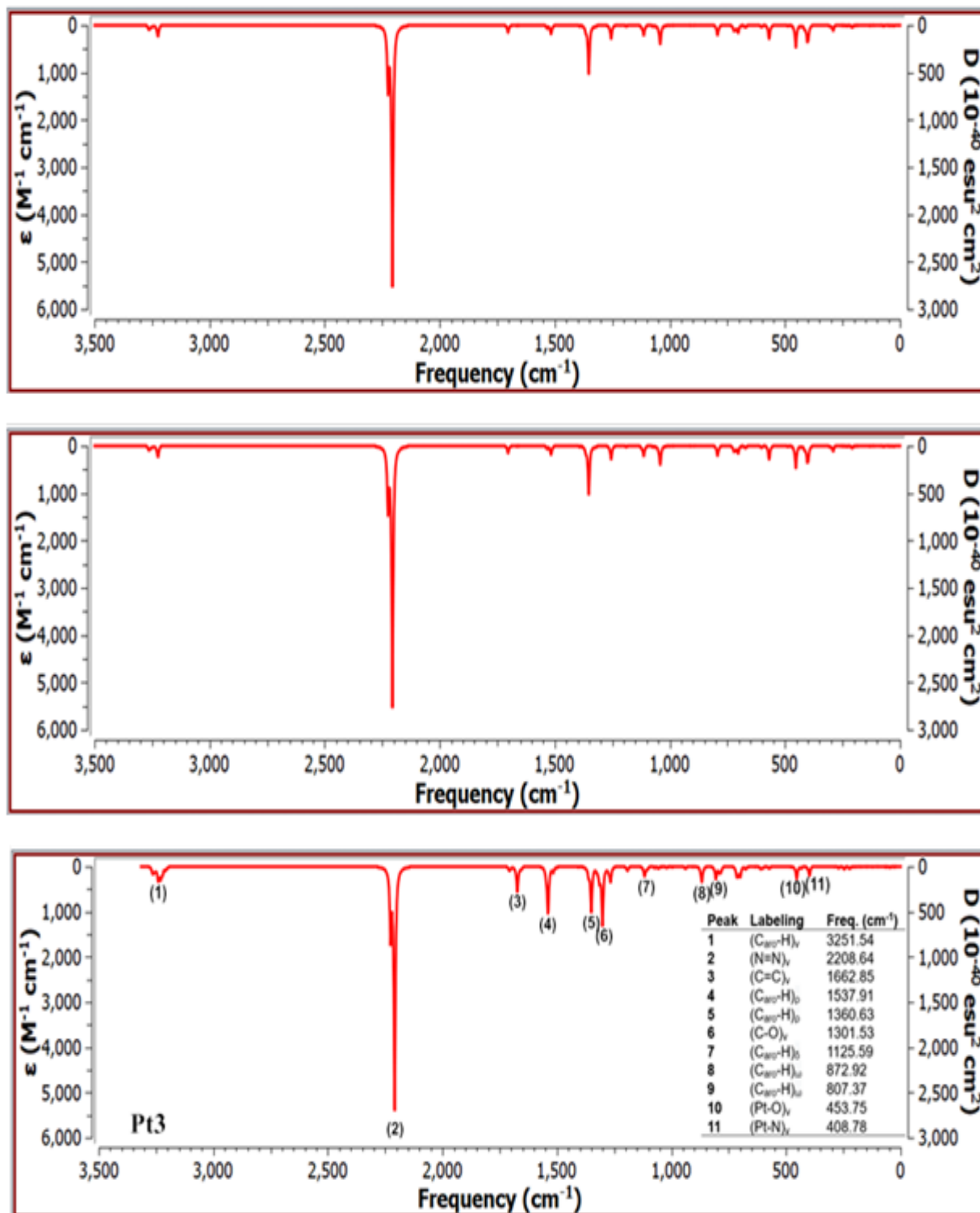


Figure 2. Calculated IR spectra of Pt1-Pt3 type complexes and labeling of characteristic peaks. (ω:Wagging, α: Scissoring, v: stretching, vas: asymmetric stretching)

Saadet KAYA, Sultan ERKAN

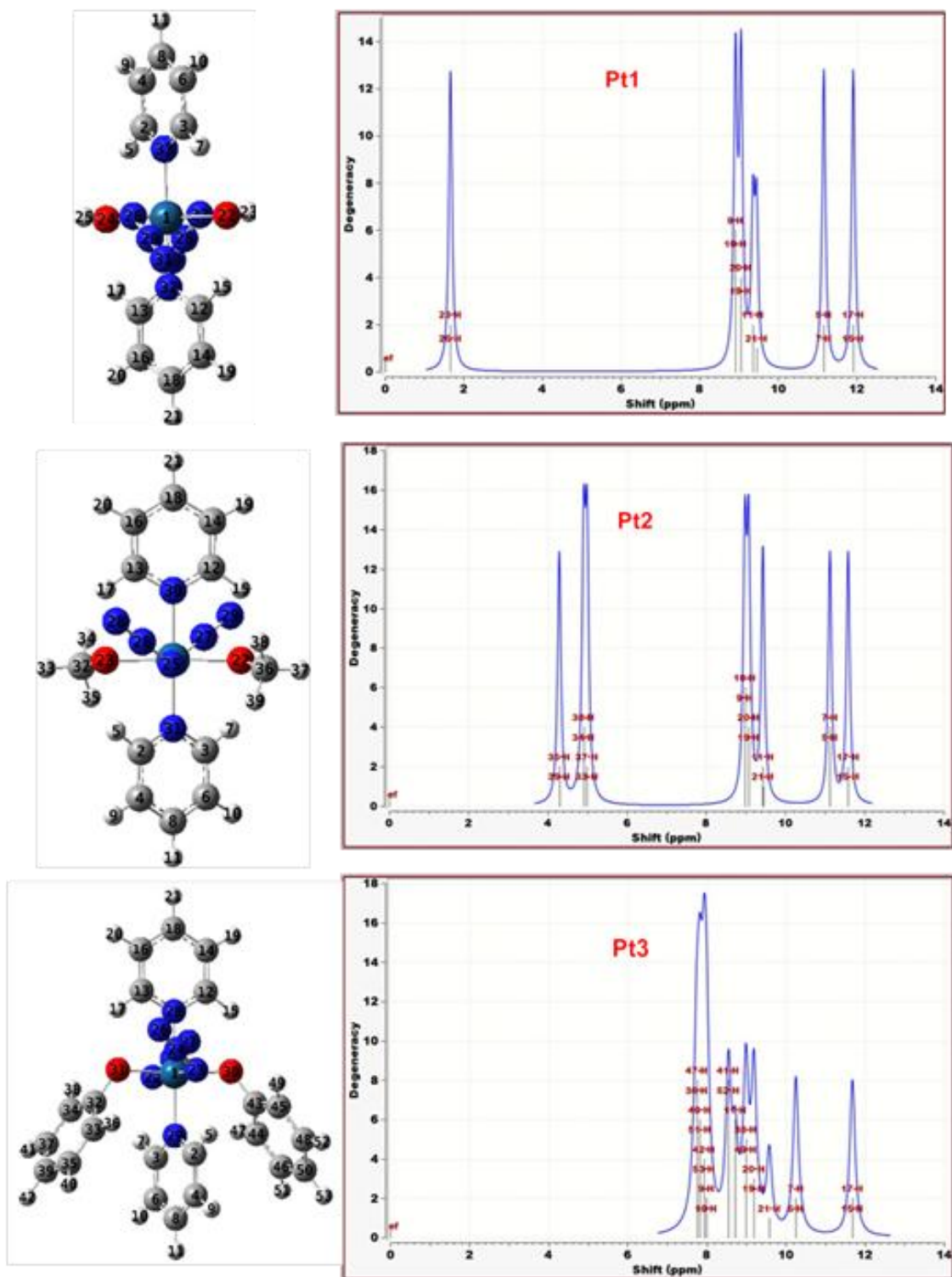


Figure 3. ^1H -NMR chemical shifts of Pt1-Pt3 complexes calculated with WB97XD/6-31G(d,p)/SDD.

This situation shows that the oxygen atoms in the molecular structure of the Pt1 complex significantly affect the hydrogens. In the spectrum in the figure, it is seen that the chemical shift values of some protons are the same and therefore they are defined

as equivalent protons. It was determined that these equivalent protons are located in trans positions. The fact that the protons are located in such a symmetric position strongly supports that the complexes have octahedral geometry. The trans

position shows that the complexes have a symmetric structure both theoretically and experimentally.

3.5. Frontier molecular orbital analyses

The highest occupied molecular orbital (HOMO) and the lowest unoccupied molecular orbital (LUMO) of molecules are called leading molecular orbitals (FMO). It is widely reported that the E_{gap} values of molecules are related to optical and electronic properties [11] and the energy gap

between leading molecular orbitals is also used to predict their properties. The energy gap (E_g) between leading molecular orbitals can be calculated from equation (1).

$$E_g = E_{LUMO} - E_{HOMO} \quad (1)$$

The contour diagrams of the leading molecular orbitals, their energies and energy gaps are given in Figure 4.

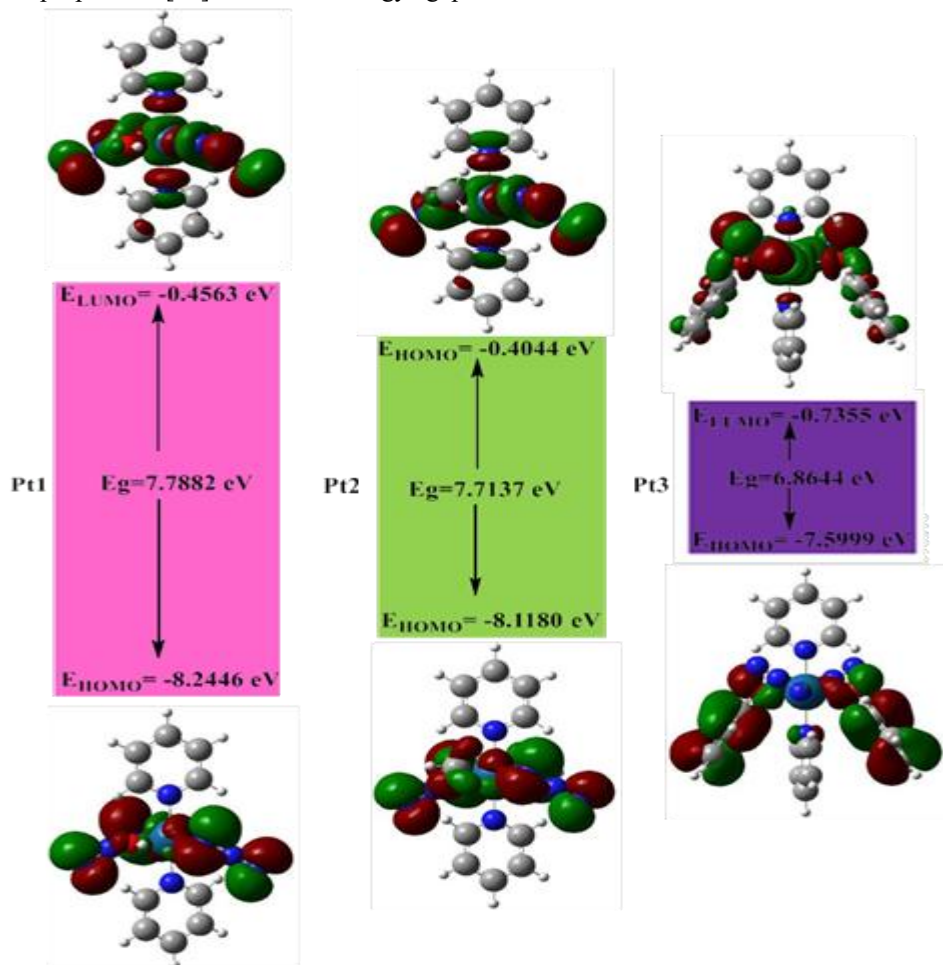


Figure 4. Contour diagrams of the calculated precursor molecular orbitals, their energies, and energy gaps of Pt(IV) type complexes.

In Pt1 and Pt2 complexes, HOMO orbitals are localized on azide ligands. This shows that the electron density of azide ligand contributes to the HOMO level. In Pt3 complex, HOMO orbitals are delocalized mostly on pyridine ligands. This shows that there is a shift in HOMO orbital structure with ligand change of Pt3.

In all complexes, LUMO orbitals are predominantly localized on azide ligands. This shows that electron deficiency is concentrated on azide ligands.

For Pt1: $E_{HOMO} = -8.2446$ eV, $E_{LUMO} = -0.4563$ eV, $E_g = 7.7882$ eV. For Pt2: $E_{HOMO} = -8.1180$ eV, $E_{LUMO} = -0.4044$ eV, $E_g = 7.7137$ eV. For Pt3: $E_{HOMO} = -7.5999$ eV, $E_{LUMO} = -0.7355$ eV, $E_g = 6.8644$ eV. These energy gaps show that the optical and electronic properties of the complexes change depending on the ligand structure and that the energy gap is smaller in the Pt3 complex. The lower energy gap indicates that Pt3 may be more active in terms of electronic transitions.

Ligand exchange has shortened the charge transition distance in the complexes and advanced to an energy range that supports the intraligand charge transfer (ILCT) mechanism. This can significantly change the electronic properties of the complexes. It is reported in the literature that ILCT increases the conductivity properties of the materials in particular and directly affects the light efficiency in OLED devices. In this context, the lower E_g value in the Pt3 complex may provide advantages in terms of OLED applications.

3.6. Molecular Electrostatic Potential (MEP) Map

Molecular electrostatic potential (MEP) maps are an important tool used to visualize the reactive regions of molecules and to understand chemical reaction mechanisms. These maps represent the electrostatic potential distribution of molecules with a color scale and present a ranking from negative to

positive. In this scale, red represents the most negative (vulnerable to nucleophilic attack) regions, orange and yellow represent less negative regions, green represents neutral regions, and blue represents the most positive (vulnerable to electrophilic attack) regions. These color distributions allow the electrostatic interactions and reactivity between molecules to be estimated. [12] The MEP maps calculated for Pt1-Pt3 complexes are given in Figure 3.10.

When looking at the MEP maps, it is seen that the electrostatic potential distribution of molecules is shown in colors and these colors play an important role in defining the reactive regions of molecules. Green colored regions represent regions with neutral potential. These areas are generally areas that provide the general balance of the molecule and do not show any significant nucleophilic or electrophilic properties.

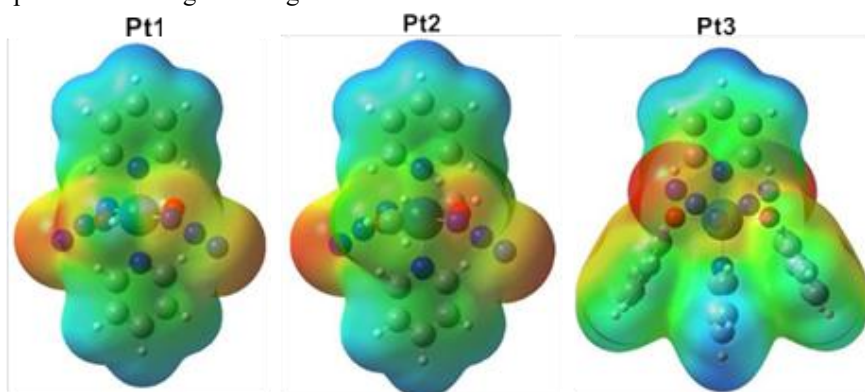


Figure 5. MEP maps of the studied complexes

These neutral regions represent the parts of the molecule that are chemically more stable and passive. Blue colored regions represent the most positive regions of molecules, i.e. most open to electrophilic attack. It is especially noteworthy that blue colored regions in complexes are concentrated on aromatic rings. This shows that aromatic rings are electron deficient areas in the molecule and are open to electrophilic reactions. These regions have the potential to establish strong interactions with electron donor groups coming from outside. Red colored regions show the most negative regions of molecules, i.e. most suitable for nucleophilic attack. Red colored regions in complexes are concentrated especially in areas where azide atoms are located. Azide groups exhibit nucleophilic properties due to their high electron densities. This indicates that

azide groups are the most active reactive areas in the molecule and can play an important role in chemical reactions. Nitrogen atoms on molecules attract attention as electron-withdrawing groups. The regions around nitrogen atoms have an important effect on the formation of the electrophilic and nucleophilic properties of the molecule. The fact that these regions are indicated in red indicates that electron density is concentrated in these areas and that these regions are suitable for nucleophilic attacks. Therefore, red regions can generally be considered as the reactive centers of the molecule. In conclusion, MEP maps provide important information in understanding the electrostatic properties and chemical reactivity of Pt1–Pt3 complexes. The distinct distribution of blue and red regions clearly reveals the reactive

regions of the molecules and provides insights into how these regions may be involved in chemical reactions. In particular, the interaction regions of azide and aromatic rings provide valuable

information about the chemical reactivity and potential biological activities of these complexes.

Table 3. Binding energies (kcal/mol) between Pt1-Pt3 complexes and target proteins 1jnx, 1x2j and 2hq6

	Pt1	Pt2	Pt3	Cis-Pt
1JNX	-218.28	-230.93	-250.49	-115.89
1X2J	-277.53	-291.55	-344.94	-121.97
2HQ6	-239.02	-253.37	-291.27	-122.28

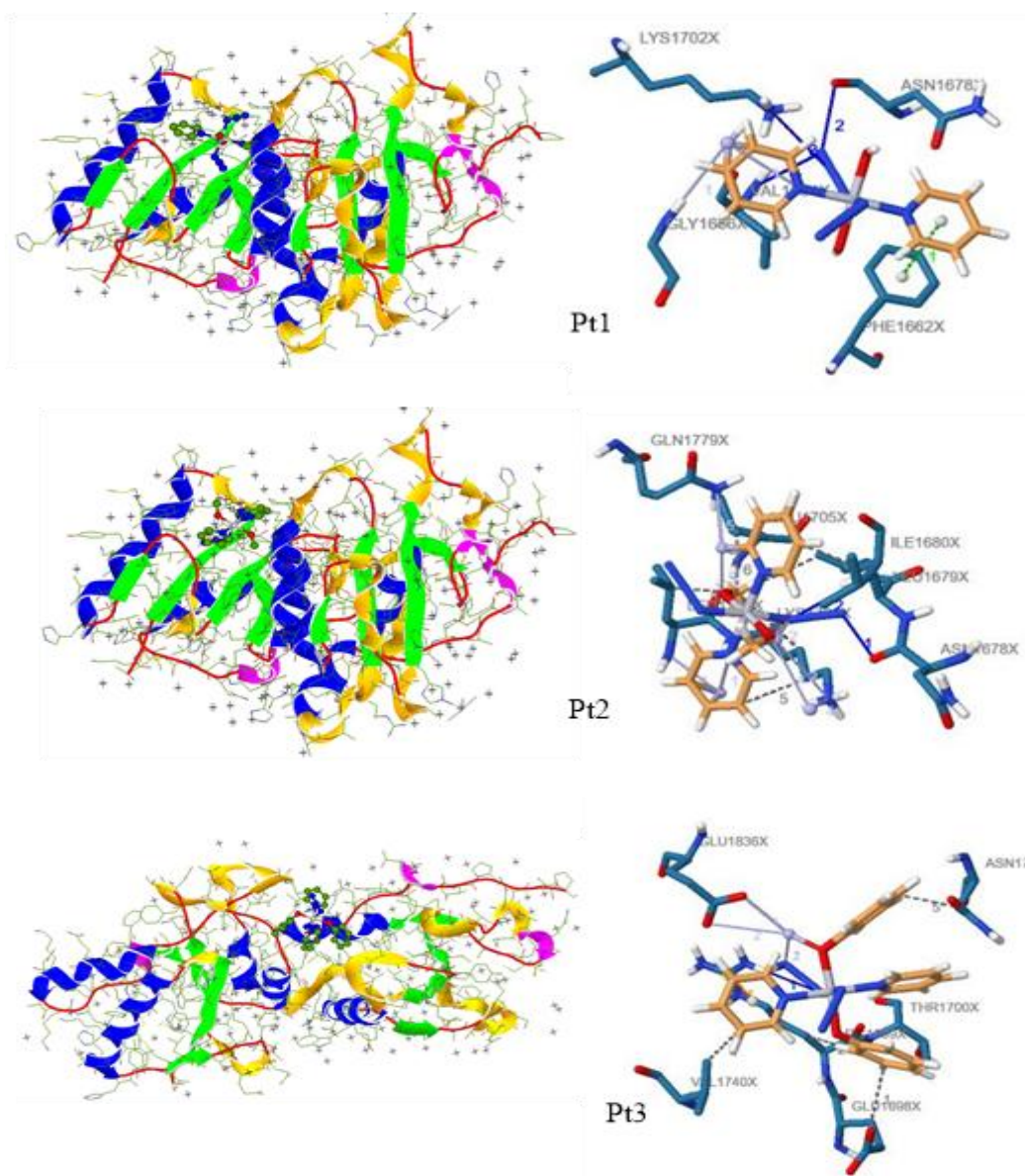


Figure 6. Binding modes and interaction types of platinum complexes docked with the 1JNX target protein

3.7. Molecular Docking

In recent years, drug modeling studies have attracted great attention. The most important

reasons for this interest in modeling studies are that they are not very costly and time-consuming. Molecular modeling is based on examining the

relationship between the molecules under study with the mechanism of action. This process is carried out in a 3D computer environment. All processes that take this basic principle into account are called molecular docking. In molecular docking studies, the chemical species is called ligand and the effect factor is called target protein. Ligands are organic and inorganic chemical species. The design of the synthesized or likely to be synthesized ligands depends entirely on the user. The functional groups in the ligands can be improved by changing the electron acceptor or electron donor groups. The activity of the synthesized or designed ligands may vary depending on the interaction strength with the target proteins. The ligand under study and the target protein should form a key-lock model and have low binding energy. This is very important in determining the theoretical effectiveness of the ligand. Therefore, the target proteins that the ligands will affect are extremely important. In this study, docking calculations were performed in the HEX 8.0.0 program. The target proteins were selected from the protein bank. PDB ID= 1JNX, Crystal structure of BRCT repeat region from breast cancer associated protein BRCA1 [13] PDB ID= 2HQ6, Colon cancer antigen, a tumor marker used in cancer diagnosis [14]. Binding energies of Pt1-Pt3 complexes with target proteins 1JNX (breast cancer), 1X2J (lung cancer) and 2HQ6 (colon cancer) are given in Table 3.

According to the data in Table 3, Pt1, Pt2 and Pt3 complexes exhibited lower binding energies for all target proteins compared to cisplatin (cis-Pt). This shows that Pt1-Pt3 complexes are more advantageous than cisplatin in terms of anticancer activity. Especially, Pt3 complex has the lowest binding energy value in all target proteins and shows the highest biological activity. Binding energies given in Table 3 show that anticancer activity increases with the exchange of auxiliary ligand. In addition, anticancer activities of Pt1-Pt3 complexes are more advantageous than cis-Pt. Binding modes and interaction types between the studied complexes and 1JNX (breast cancer), 1X2J (lung cancer) and 2HQ6 (colon cancer) target proteins are given in Figures 6-8.

Hydrogen bonds are strong secondary chemical interactions that play a critical role in ensuring the stability of the binding positions between the protein and the ligand. Pt1, Pt2, and Pt3 complexes

contribute to the decrease of binding energies and the stabilization of the ligand in the binding site by forming hydrogen bonds with the target proteins. In the Pt1 complex, hydrogen bonds were formed with the amino acid residues GLY-146, ALA-148, and SER-149 in the 1JNX protein. The distance of the hydrogen bonds varied between 2.72–3.30 Å. These amino acid residues in the binding site supported the tight binding of the ligand to the protein surface. In the Pt2 complex, hydrogen bonds were observed with the residues GLU-146, SER-150, and GLY-152 in the 1X2J protein. The distance of the hydrogen bonds was measured in the range of 2.89–3.36 Å. These bonds increased the stability of Pt2 in the binding site and made a significant contribution to the binding energy. The Pt3 complex formed hydrogen bonds with ARG-75, GLN-112 and GLU-76 amino acid residues in the 2HQ6 protein. The distances of the hydrogen bonds varied between 2.86–3.45 Å. The hydrogen bond formed especially with ARG-75 increased the binding stability by ensuring that the ligand tightly binds to the protein. Hydrophobic interactions are another important secondary chemical force supporting the binding stability between the protein and the ligand. These interactions are formed by the interaction of hydrophobic amino acids on the protein surface with the ligand and ensure that the ligand remains in close proximity to the protein. For the Pt1 complex, hydrophobic interactions were observed especially with the amino acid residues PRO-33 and ALA-102. The hydrophobic interaction distances varied between 3.35–3.55 Å. These interactions enabled the Pt1 complex to take a more stable position in the binding site. For the Pt2 complex, hydrophobic interactions were observed with amino acid residues LEU-142 and GLU-146. The hydrophobic interaction distances were measured in the range of 3.62–3.76 Å. These interactions contributed to the stability by supporting the binding of Pt2 to the protein surface. For the Pt3 complex, hydrophobic interactions were observed with amino acid residues VAL-76, ALA-102, and GLU-112. The distances of these interactions varied between 3.38–3.74 Å. The density of hydrophobic interactions in the Pt3 complex made a significant contribution to the binding energy and increased the stability in the binding site. Hydrogen bonds and hydrophobic interactions are the main factors determining the

Saadet KAYA, Sultan ERKAN

binding modes and stability of Pt1, Pt2, and Pt3 complexes to target proteins. Especially, amino acid residues such as ALA, GLY, LEU, GLU, and VAL played an important role in the interaction with ligands and contributed to the binding energies. The intense hydrogen bonds and hydrophobic interactions observed in the Pt3

complex reveal that this complex exhibits the highest binding stability to target proteins and is the most advantageous in terms of biological activity. These findings are an important guide in understanding the interaction mechanisms of platinum complexes with biological targets.

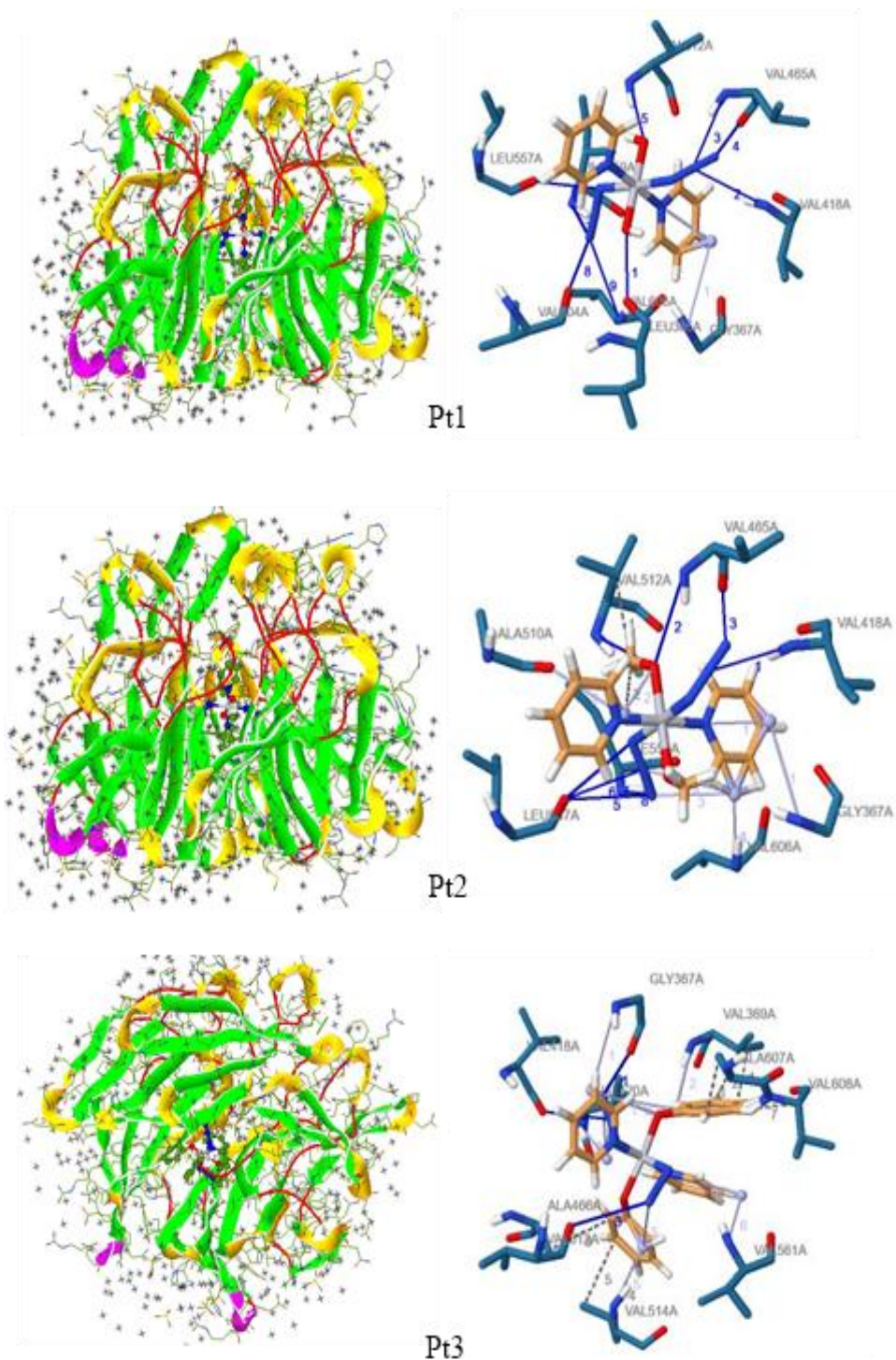


Figure 7. Binding modes and interaction types of platinum complexes docked with the 1X2J target protein

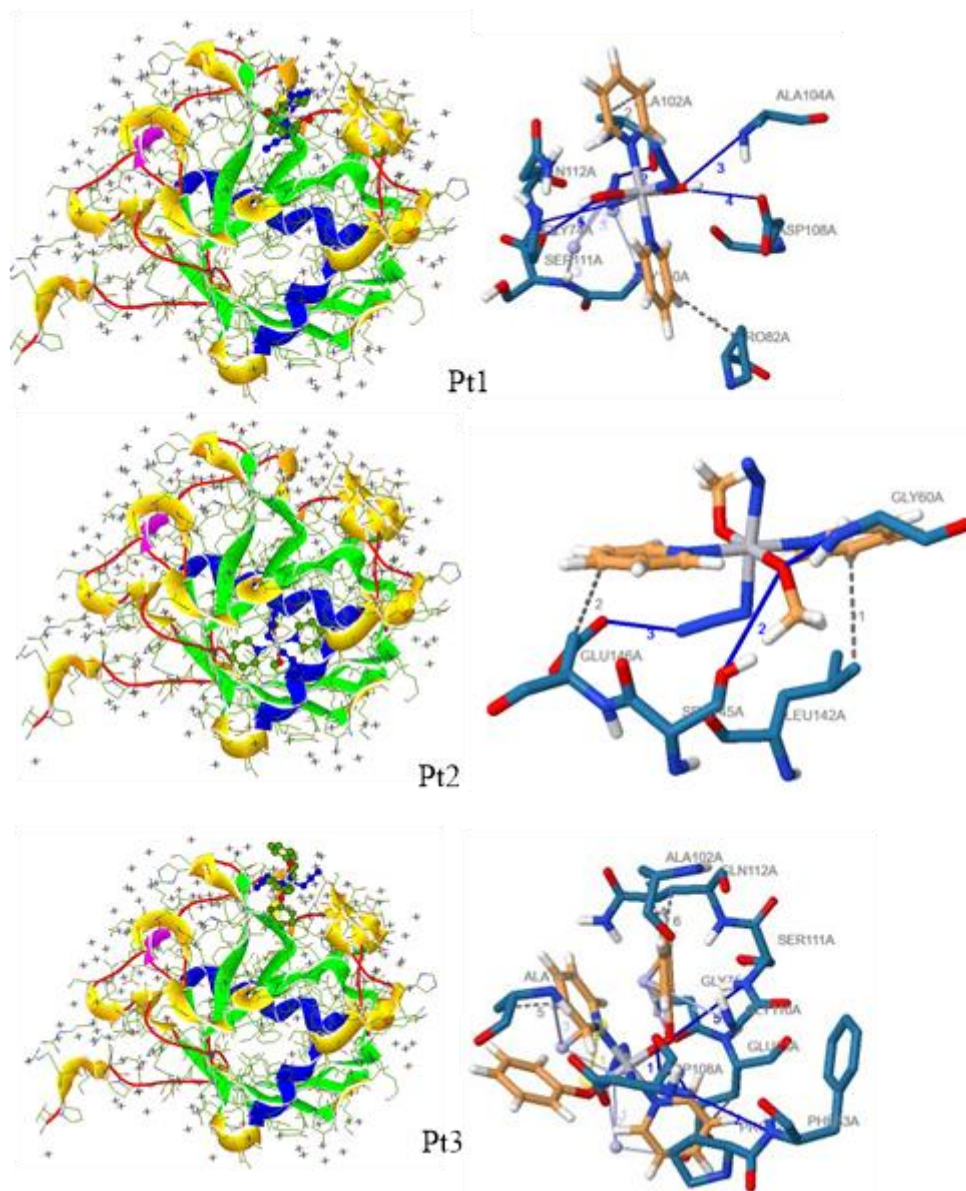


Figure 8. Binding modes and interaction types of platinum complexes docked with the 2HQ6 target protein

4. Conclusions

This study comprehensively analyzed the structural, electronic and biological properties of Pt1, Pt2 and Pt3 complexes using computational chemistry methods. The WB97XD/6-31G(d,p)/SDD method was determined as the most suitable calculation level for Pt1, Pt2 and Pt3 complexes. The optimized structures of the complexes showed that the central platinum atom has an octahedral geometry and the bond lengths and bond angles exhibit symmetrical features. The high agreement between the experimental and calculated structural parameters supports the accuracy and reliability of the methods used. IR and $^1\text{H-NMR}$ spectra characterized the molecular structures of the complexes in detail. In the IR

spectra, the characteristic bond strains of azide ligands and vibrational modes of aromatic rings were clearly observed. $^1\text{H-NMR}$ analyses confirmed that the chemical shift values of protons in the complexes were consistent with the molecular structure and that the complexes exhibited trans-octahedral symmetry. HOMO and LUMO analyses elucidated the optical and electronic properties of Pt1, Pt2 and Pt3 complexes and showed that the energy gaps (E_g) changed depending on the ligand structure. The lower energy gap of Pt3 complex indicates a higher activity potential in terms of electronic transitions. The observation of intraligand charge transfer (ILCT) mechanisms provides a promising finding for the potential use of the complexes in

optoelectronic applications. Molecular electrostatic potential (MEP) maps clearly defined the nucleophilic and electrophilic regions of the complexes. The red (negative) regions revealed the nucleophilic properties of azide ligands and the blue (positive) regions revealed the electrophilic nature of aromatic rings. This potential distribution in the reactive regions of the complexes provides an important guide to understand their interactions with biological targets. Docking studies showed that Pt1, Pt2 and Pt3 complexes exhibited strong interactions with breast cancer (1JNX), lung cancer (1X2J) and colon cancer (2HQ6) proteins. The Pt3 complex stood out as the most advantageous complex in terms of biological activity, exhibiting the lowest binding energies and intense hydrogen bonding and hydrophobic interactions. All complexes showed higher binding stability and anticancer activity compared to the reference cisplatin (cis-Pt).

References

- [1] Zheng, Y. R., Suntharalingam, K., Johnstone, T. C., & Lippard, S. J. (2015). Encapsulation of Pt (IV) prodrugs within a Pt (II) cage for drug delivery. *Chemical science*, 6(2), 1189-1193.
- [2] Sánchez-Camacho, J., Infante-Tadeo, S., Carrasco, A. C., Scoditti, S., Martínez, Á., Barroso- Bujans, F., ... & Salassa, L. (2023). Flavin-conjugated Pt (IV) anticancer agents. *Inorganic Chemistry*, 62(14), 5644-5651.
- [3] Barth, M. C., Häfner, N., Runnebaum, I. B., & Weigand, W. (2023). Synthesis, Characterization and Biological Investigation of the Platinum (IV) Tolfenamato Prodrug-Resolving Cisplatin-Resistance in Ovarian Carcinoma Cell Lines. *International Journal of Molecular Sciences*, 24(6), 5718.
- [4] Kenny, R. G., Chuah, S. W., Crawford, A., & Marmion, C. J. (2017). Platinum (IV) prodrugs—a step closer to Ehrlich's vision?. *European Journal of Inorganic Chemistry*, 2017(12), 1596-1612.
- [5] Zhou, Z., Shi, P., Wang, C., Sun, Y., & Gao, C. (2024). Recent updates in nanoscale delivery systems of platinum (IV) antitumor prodrugs. *Coordination Chemistry Reviews*, 508, 215774.
- [6] Dikova, Y. M., Yufit, D. S., & Williams, J. G. (2023). Platinum (IV) Complexes with Tridentate, NNC-Coordinating Ligands: Synthesis, Structures, and Luminescence. *Inorganic Chemistry*, 62(4), 1306-1322.
- [7] Farrer, N. J., Woods, J. A., Salassa, L., Zhao, Y., Robinson, K. S., Clarkson, G., ... & Sadler, P. J. (2010). A potent trans-diimine platinum anticancer complex photoactivated by visible light. *Angewandte Chemie*, 47(122), 9089-9092.
- [8] Novohradsky, V., Pracharova, J., Kasparkova, J., Imberti, C., Bridgewater, H. E., Sadler, P. J., & Brabec, V. (2020). Induction of immunogenic cell death in cancer cells by a photoactivated platinum (IV) prodrug. *Inorganic chemistry frontiers*, 7(21), 4150-4159.
- [9] Yanai, T., Tew, D. P., & Handy, N. C. (2004). A new hybrid exchange–correlation functional using the Coulomb-attenuating method (CAM-B3LYP). *Chemical Physics Letters*, 393(1-3), 51-57.
- [10] Ditchfield, R., Hehre, W. J., & Pople, J. A. (1971). Self-consistent molecular orbital methods. IX. An extended Gaussian-type basis for molecular-orbital studies of organic molecules. *Journal of Chemical Physics*, 54(2), 724-728.
- [11] Andrae, D., Häußermann, U., Dolg, M., Stoll, H., & Preuß, H. (1990). Energy-adjusted ab initio pseudopotentials for the second and third row transition elements. *Theoretical Chemistry Accounts*, 77(2), 123-141.
- [12] Ohtomo, Y., Ishiwata, K., Hashimoto, S., Kuroiwa, T., & Tahara, K. (2021). Revisiting Dehydrothiopheno [12] annulenes: Synthesis, Electronic Properties, and Aromaticity. *The Journal of Organic Chemistry*, 86(19), 13198-13211.
- [13] Khalid, H. H., Erkan, S., & Bulut, N. (2021). Halogens effect on spectroscopy, anticancer and molecular docking studies for platinum complexes. *Optik*, 244, 166324.
- [14] Kaya, S., Erkan, S., & Karakaş, D. (2021). Computational investigation of molecular

structures, spectroscopic properties and antitumor-antibacterial activities of some Schiff bases. *Spectrochimica Acta Part A: Molecular and Biomolecular Spectroscopy*, 244, 118829.

- [15] Padmanabhan, B., Tong, K. I., Ohta, T., Nakamura, Y., Scharlock, M., Ohtsuji, M., ... & Yamamoto, M. (2006). Structural basis for defects of Keap1 activity provoked by its point mutations in lung cancer. *Molecular cell*, 21(5), 689-700.
- [16] Davis, T. L., Walker, J. R., Campagna-Slater, V., Finerty Jr, P. J., Paramanathan, R., Bernstein, G., ... & Dhe-Paganon, S. (2010). Structural and biochemical characterization of the human cyclophilin family of peptidyl-prolyl isomerases. *PLoS biology*, 8(7), e1000439.